Organic Syntheses

Palladium-Catalyzed Hydrodefluorination of Fluoroarenes

Joseph J. Gair, Ronald L. Grey*, Simon Giroux, and Michael A. Brodney

Vertex Pharmaceuticals Inc, 50 Northern Avenue, Boston, Massachusetts 02210, United States

Checked by Vincent Porte, Daniel Kaiser, and Nuno Maulide

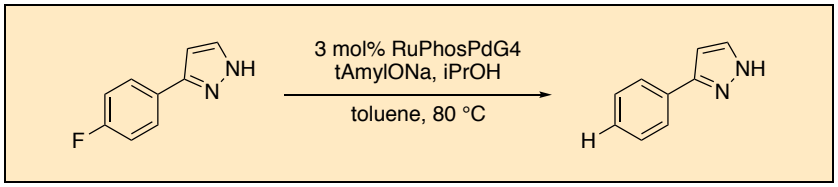

Procedure (Note 1)

3-Phenyl-1H-pyrazole. An oven dried 250-ml, three-necked, round-bottomed flask equipped with a Teflon-coated magnetic stir bar (3 cm) is charged with 3-(4-fluorophenyl)-1*H*-pyrazole (6.49 g, 40.0 mmol, 1.00 equiv) (Note 2) and RuPhos Palladacycle Gen. 4 (1.02 g, 1.20 mmol, 3.00 mol%) (Note 3). The vessel is equipped with an oven-dried reflux condenser and capped with two rubber septa. The reflux condenser is equipped with an argon inlet attached to a Schlenk line. The apparatus is evacuated, refilled with argon (3x). Toluene (55 mL, 0.73M) (Note 4) is added in two portions at room temperature via syringe through the side arm of the three-necked flask under flow of argon. The flask is charged with 2-propanol (15.3 mL, 200 mmol, 5.00 equiv) (Note 5) at room temperature via syringe through the side arm of the three-necked flask. The yellow suspension is stirred for five min under positive argon pressure. The resulting yellow solution (Figure 1A) is treated with a solution of sodium *tert*-pentoxide in toluene (30 mL, 3.3M, 100 mmol, 2.5 equiv) (Note 6) under flow of argon (exothermic reaction). The resulting black suspension (Figure 1B) is transferred to an aluminum heating block equilibrated to 80 °C. Water is circulated through the reflux condenser.

Published on the Web 5/19/2021

A thermometer is inserted through one neck, replacing one of the septa, and the reaction is stirred at 80 °C (internal temperature = 70 °C) under argon atmosphere (Figure 1C). After 18 h, ^{1}H and ^{19}F NMR showed no evidence of starting material (Note 7).

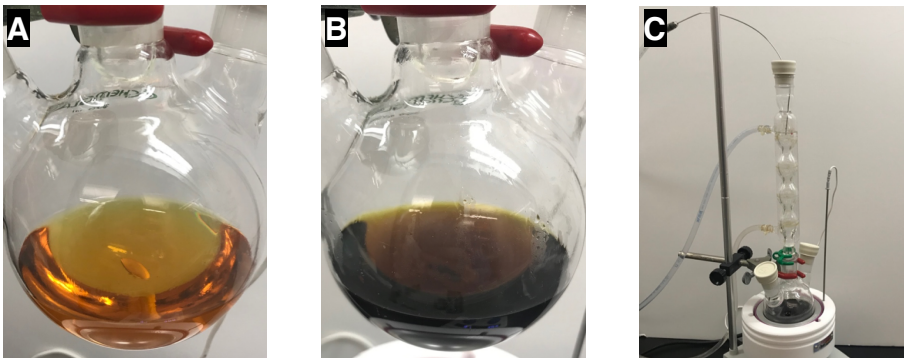

Figure 1. (A) Reaction mixture prior to addition of sodium *tert*-pentoxide; (B) Reaction mixture immediately after adding sodium tert-pentoxide; and (C) Reaction setup during heating

The black heterogeneous reaction mixture is removed from the heating block and allowed to cool to room temperature (Figure 2A). The reaction mixture is filtered through a pad of sand (1 cm) layered with Celite (20 g) on a fritted funnel (porosity 2) into a 500-mL round-bottomed flask (Figure 2B). The filter cake is carefully triturated with a spatula to insure a better filtration. The reaction vessel and Celite cake are then washed with ethyl acetate until the eluent is colorless (9 x 20 mL). The filtrate is concentrated by rotary evaporation (50 °C, 70 mmHg) to afford a thick brown paste (Figure 2C).

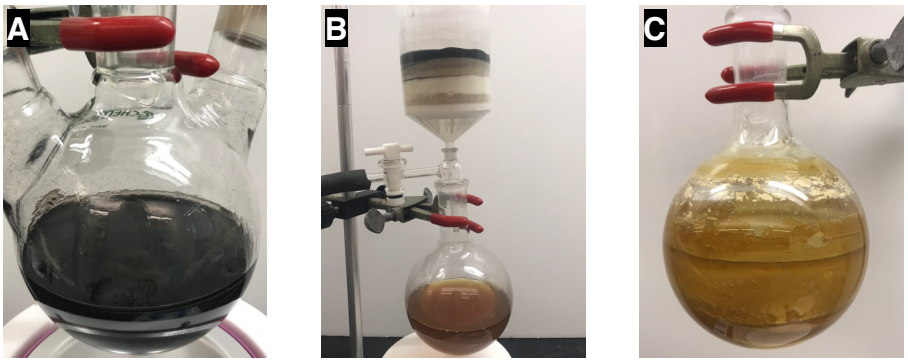

Figure 2. (A) Heterogeneous reaction mixture after heating for 18 hours; (B) Reaction mixture after filtration through Celite; and (C) Filtrate after concentration by rotary evaporation

The concentrated crude material is quenched with saturated aqueous sodium bicarbonate (40 mL) at room temperature. The resulting slurry is suspended with swirling and transferred via plastic funnel to a 125-mL separatory funnel. The round-bottomed flask containing quenched material is washed with a biphasic mixture of deionized water (5 mL) and dichloromethane (5 mL) (5 x biphasic wash) to transfer any residual product to the separatory funnel. The separatory funnel is shaken and the layers (Figure 3A) are allowed to separate over five min. The dichloromethane layer is collected in a 250 mL Erlenmeyer flask, and the aqueous layer is re-extracted with dichloromethane (4 x 20 mL) until the organic phase is colorless (Figure 3B,C). The organic fractions are treated with sodium sulfate (20 g), left to dry for 10 min and clarified by vacuum filtration on a fritted funnel into a 500-mL round-bottomed flask. The drying agent is washed with ethyl acetate (3 x 40 mL) to extract any residual product and the ethyl acetate washes are filtered into the dichloromethane filtrate. The combined filtrates are charged with Celite (17 g) and concentrated by rotary evaporation (50 °C, 70 mmHg).

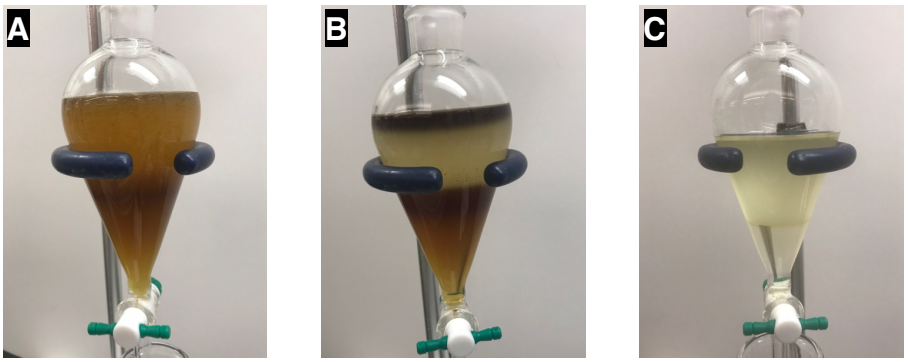

Figure 3. (A) Biphasic mixture after transferring to separatory funnel and shaking; (B) Biphasic mixture after second extraction with dichloromethane; and (C) Biphasic mixture after fourth extraction with dichloromethane

A glass chromatography column (inner diameter 5 cm) is charged with silica gel (200g) (Note 8) loaded as a slurry with 40 vol% ethyl acetate in *n*-heptane. The silica gel slurry is allowed to settle, and excess mobile phase is eluted by gravity. Atop the silica gel slurry is loaded the crude solid adsorbed on Celite followed by a layer of sand (4 cm). The packed column is then eluted with 40 vol% ethyl acetate in *n*-heptane (1L) followed by ethyl acetate (1L) (Note 9). The eluent is collected in 25 x 150 mm test tubes (50 mL fractions) for 40 fractions. Fractions 13–28 contain the desired product (Note 10) and are concentrated by rotary evaporation (50 °C, 50 mmHg) in a 500-mL round-bottomed flask. Thick oil is dissolved with EtOAc and transferred to a 50-mL round-bottomed flask and concentrated under reduced pressure to yield the desired product (5.70 g) as a tan solid in >90% purity as assayed by ^{1}H NMR (Figure 4A).

The chromatographed material is further purified by crystallization (Note 11): The solid is transferred to a tared 30-mL vial as a solid, and any residual material in the 500-mL round-bottomed flask is transferred by washing with hot benzene (4 x 2 mL, 70 °C) followed by pipette transfer to the 30-mL vial. The tan solid suspended in benzene is dissolved by heating the vial (aluminum heating block, 90 °C) until the mixture is gently refluxing (5 min reflux with intermittent swirling). The resulting, hazy orange mixture (Figure 4B) is layered with *n*-heptane (8 mL) (Figure 4C) and allowed to cool to room temperature over 4 h (Note 12) (Figure 4D). The recrystallization setup is then gently swirled to facilitate mixing of the benzene and *n*-heptane

layers. The recrystallization setup is stored for 24 h at 4 °C, which affords large colorless crystals (Figure 4E). The supernatant is removed by pipette. The colorless crystals are washed with cold *n*-heptane (2 x 6 mL, 4 °C) and dried first by rotary evaporation (40 °C, 10 mmHg) then in a vacuum oven (30 °C, 0.1 mmHg, 4 h) to afford 3-phenyl-1H-pyrazole (5.06 g, 88% yield (4.97 g, 86% based on purity)) as a colorless solid (Figure 4F) (Notes 13 and 14).

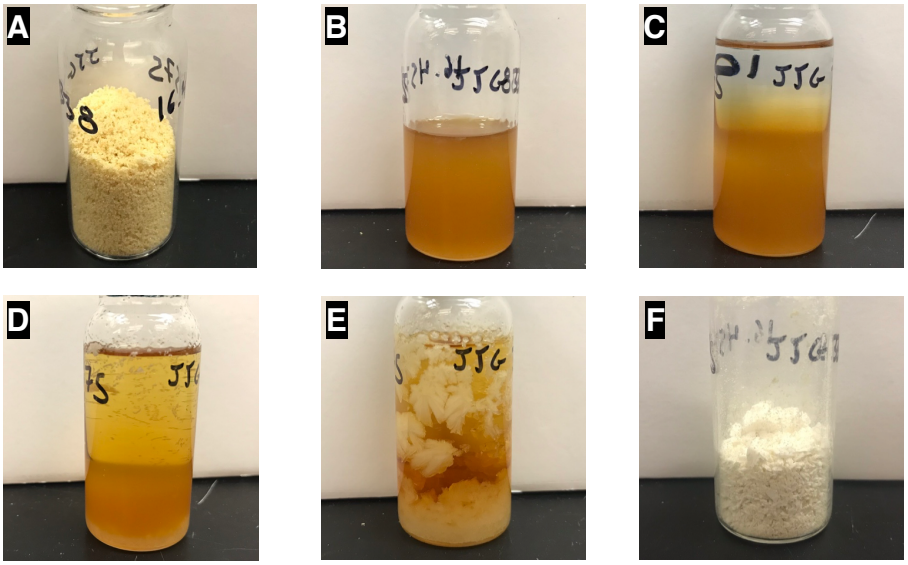

Figure 4. (A) Tan material obtained from column chromatography; (B) Concentrated solution of desired product in hot benzene; (C) After layering with hot *n*-heptane; (D) Small crystals formed after cooling to room temperature; (E) Large crystals after cooling for 24 h at 4 °C; and (F) Isolated colorless crystalline solid

Notes

1. Prior to performing each reaction, a thorough hazard analysis and risk assessment should be carried out with regard to each chemical substance and experimental operation on the scale planned and in the context of the laboratory where the procedures will be carried out. Guidelines for carrying out risk assessments and for analyzing the hazards associated

with chemicals can be found in references such as Chapter 4 of "Prudent Practices in the Laboratory" (The National Academies Press, Washington, D.C., 2011; the full text can be accessed free of charge at https://www.nap.edu/catalog/12654/prudent-practices-in-the-laboratory-handling-and-management-of-chemical. See also "Identifying and Evaluating Hazards in Research Laboratories" (American Chemical Society, 2015) which is available via the associated website "Hazard Assessment in Research Laboratories" at https://www.acs.org/content/acs/en/about/governance/committees/chemicalsafety/hazard-assessment.html. In the case of this procedure, the risk assessment should include (but not necessarily be limited to) an evaluation of the potential hazards associated with 3-(4-fluorophenyl)-1*H*-pyrazole, RuPhos Palladacycle Gen. 4, 2-propanol, sodium *tert*-pentoxide, toluene, ethyl acetate, sodium bicarbonate, dichloromethane, sodium sulfate, *n*-heptane, celite, silica gel, benzene, acetonitrile, trifluoroacetic acid, and deuterated chloroform.

2. 3-(4-Fluorophenyl)-1H-pyrazole (>97%) was obtained from Alfa Aesar (H34355) as an off-white powder and used as received.
3. RuPhos Palladacycle Gen. 4 (>98%) was obtained from Strem Chemicals (46-0395) as a beige powder and used as received.
4. Toluene (anhydrous, 99.8%) was purchased from Sigma Aldrich (244511) in a Sure/Seal bottle and used as received. Toluene was taken up from the Sure/Seal bottle via syringe under positive argon pressure.
5. 2-Propanol (>99.5%) was purchased from Sigma Aldrich (I9516) and used as received. 2-Propanol was measured and handled under air with no precautions to omit oxygen or moisture. Reactions conducted with lower concentrations of *i*-PrOH gave slower and sometimes incomplete conversion.
6. Sodium *tert*-pentoxide solution (40%) in toluene was purchased from Sigma Aldrich (752096) in a Sure/Seal bottle and used as received. Sodium *tert*-pentoxide was taken up from the Sure/Seal bottle via syringe under positive argon pressure. Reactions conducted with lower concentrations of sodium *tert*-pentoxide gave slower and sometimes incomplete conversion.
7. The submitters monitored reaction progress using LCMS: Reactions were monitored by liquid chromatography mass spectrometry (LCMS) on a Waters Acquity UPLC with Waters Acquity HSS T3 C18 column (2.1 mm x 50 mm) and eluting with a gradient from 10–60% acetonitrile

in water (0.1% trifluoroacetic acid modifier) over 1.6 min (product R_t= 0.80 min, starting material R_t =0.84 min).

8. Silica gel (pore size 60Å, 230-400 mesh particle size) was purchased from Sigma-Aldrich (227196). The checkers used silica gel purchased from Macherey-Nagel (particle size 0.040–0.063 mm), which was used as received.
9. Thin layer chromatography (TLC) of starting material (left lane, R_f 0.32), reaction mixture (center lane), and product (right line R_f, 0.34) on silica gel 60 (Merck KGaA) eluting with 40 vol% ethyl acetate in *n*-heptane (Figure 5). The reaction mixture is monitored by ^{1}H and ^{19}F NMR or LCMS (Note 7). Reaction monitoring by TLC is not recommended due to poor separation of starting material and product.

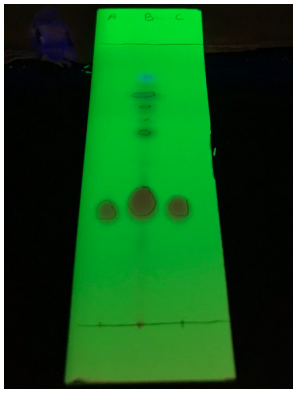

Figure 5. TLC of starting material (left lane), reaction mixture (center lane), and product (right lane)

10. Thin layer chromatography (TLC) on Silicagel 60 (Merck KGaA) eluting with 40vol% ethyl acetate in n-heptane showing fractions 1-30 from column chromatography (Figure 6).

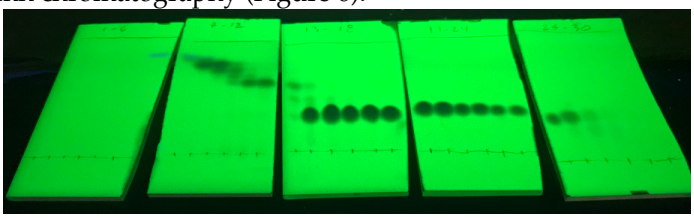

Figure 6. TLC of fractions 1-30 from column chromatography

11. An alternative crystallization procedure is reported here: To the round-bottomed flask, fitted with a condenser containing the chromatographed material was added 8 mL of benzene, and the resulting slurry was heated with intermitting swirling until all material had dissolved. To the orange mixture was added 8 mL of heptane and mixture was heated to reflux for 5 min. The mixture was allowed to return to room temperature, left standing at this temperature for 15 h, before being cooled with an ice bath (0 °C) to induce crystallization. The supernatant was removed, the crystals were washed with heptane (2 x 6 mL) and dried first by rotary evaporation (50 ℃, 10 mmHg) then with under high vacuum for 7 h.
12. The submitters observed the formation of crystals at this point, while the checkers only observed crystal formation upon subsequent cooling in the fridge.
13. Analytical data for 3-phenyl-1H-pyrazole as follows: mp 77–79 °C; IR (neat) 3166, 2962, 1456, 1353, 1071, 1046, 954, 931 cm^{-1}. ^{1}H NMR (400 MHz, $CDCl_3$, 0.7M) δ: 6.63 (d, J = 2.2 Hz, 1H), 7.32–7.44 (m, 3H), 7.61 (d, J = 2.2 Hz, 1H), 7.80 (d, br, J = 7.3 Hz, 2H), 13.01 (s, br, 1H). ^{13}C NMR (100 MHz, $CDCl_3$, 0.7M) δ: 102.7, 126.0 (2C), 128.1, 128.9 (2C), 132.4, 133.4 (br), 149.3 (br). HRMS (*m*/*z*) calcd for $C_9H_9N_2$ $[M+H]^+$: 145.0760, found: 145.0757. Purity was assessed at 98.3% by qNMR using 11.1 mg of the product and 1,3,5-trimethoxybenzene (9.1 mg) as an internal standard.
14. The checkers performed a second reaction on half scale, yielding 2.56 g (89%) of the product, while a second reaction performed by the submitters on full scale afforded 5.20 g (90% yield) of 3-phenyl-1H-pyrazole.

Working with Hazardous Chemicals

The procedures in *Organic Syntheses* are intended for use only by persons with proper training in experimental organic chemistry. All hazardous materials should be handled using the standard procedures for work with chemicals described in references such as "Prudent Practices in the Laboratory" (The National Academies Press, Washington, D.C., 2011; the full text can be accessed free of charge at http://www.nap.edu/catalog.php?record_id=12654). All chemical waste should be disposed of in accordance with local regulations. For general

guidelines for the management of chemical waste, see Chapter 8 of Prudent Practices.

In some articles in *Organic Syntheses*, chemical-specific hazards are highlighted in red "Caution Notes" within a procedure. It is important to recognize that the absence of a caution note does not imply that no significant hazards are associated with the chemicals involved in that procedure. Prior to performing a reaction, a thorough risk assessment should be carried out that includes a review of the potential hazards associated with each chemical and experimental operation on the scale that is planned for the procedure. Guidelines for carrying out a risk assessment and for analyzing the hazards associated with chemicals can be found in Chapter 4 of Prudent Practices.

The procedures described in *Organic Syntheses* are provided as published and are conducted at one's own risk. *Organic Syntheses, Inc.*, its Editors, and its Board of Directors do not warrant or guarantee the safety of individuals using these procedures and hereby disclaim any liability for any injuries or damages claimed to have resulted from or related in any way to the procedures herein.

Discussion

Fluorine plays an important role in drug discovery due to its ability to fine tune the physiochemical and metabolic properties of biologically active compounds.[2] Given the important impacts that a single fluorine substituent can have on key properties (both beneficial and detrimental), drug discovery teams frequently encounter situations in which direct comparison of fluoro- and des-fluoro-analogues is insightful. Preparation of des-fluoro-analogues typically requires lengthy resynthesis from des-fluoro building blocks. A method for direct conversion of fluorinated compounds to des-fluoro-analogues by hydrodefluorination would circumvent this resynthesis and thereby provide a useful tool to accelerate drug discovery.

Transition metal-catalyzed hydrodefluorination methodology has undergone significant growth in recent years; however, these advances have not yet translated to reliable tools for drug discovery.[3] This gap is likely a consequence of the fact that many of the reported methods are optimized for substrates with activated polyfluoro-arenes[4] or lacking functional groups (especially heterocycles) encountered in drug discovery.[5] To close this gap, we recently reported a general method for hydrodefluorination of

(hetero)arenes that is suitable for immediate implementation in drug discovery settings by virtue of the fact that the method requires only commercially available catalysts and reagents, can be set up under air and affords good yields on a variety of functional groups and heterocycles encountered in drug discovery.[6]

The substrate scope for a set of general reaction conditions suitable for hydrodefluorination of a variety of heterocyclic scaffolds is provided in Table 1. The reaction is compatible with ortho, meta, and para-substituted fluoroarenes (**1**-**4**). The reaction proceeds efficiently for substrates bearing acidic and phenolic functionality (**5**, **16**, **24**, and **26**) and NH fragments in amides (**1** and **7**), pyrazole (**3**), indazoles (**4** and **10**), imidazoles (**12**-**14**), azaindole (**17**), and secondary amines (**21** and **25**). The reaction also tolerates the presence of Lewis basic functional that might coordinate to transition metal catalysts including tertiary anilines (**2**), benzimidazoles (**8** and **9**), benzotriazole (**15**), (iso)quinolines (**18** and **19**), and pyridines (**20**-**23**). Due to its expanded scope and compatibility with a variety of functional groups encountered in medicinal chemistry, this method is well suited for immediate implementation in drug discovery settings.

Table 1. Substrate scope in palladium-catalyzed hydrodefluorination

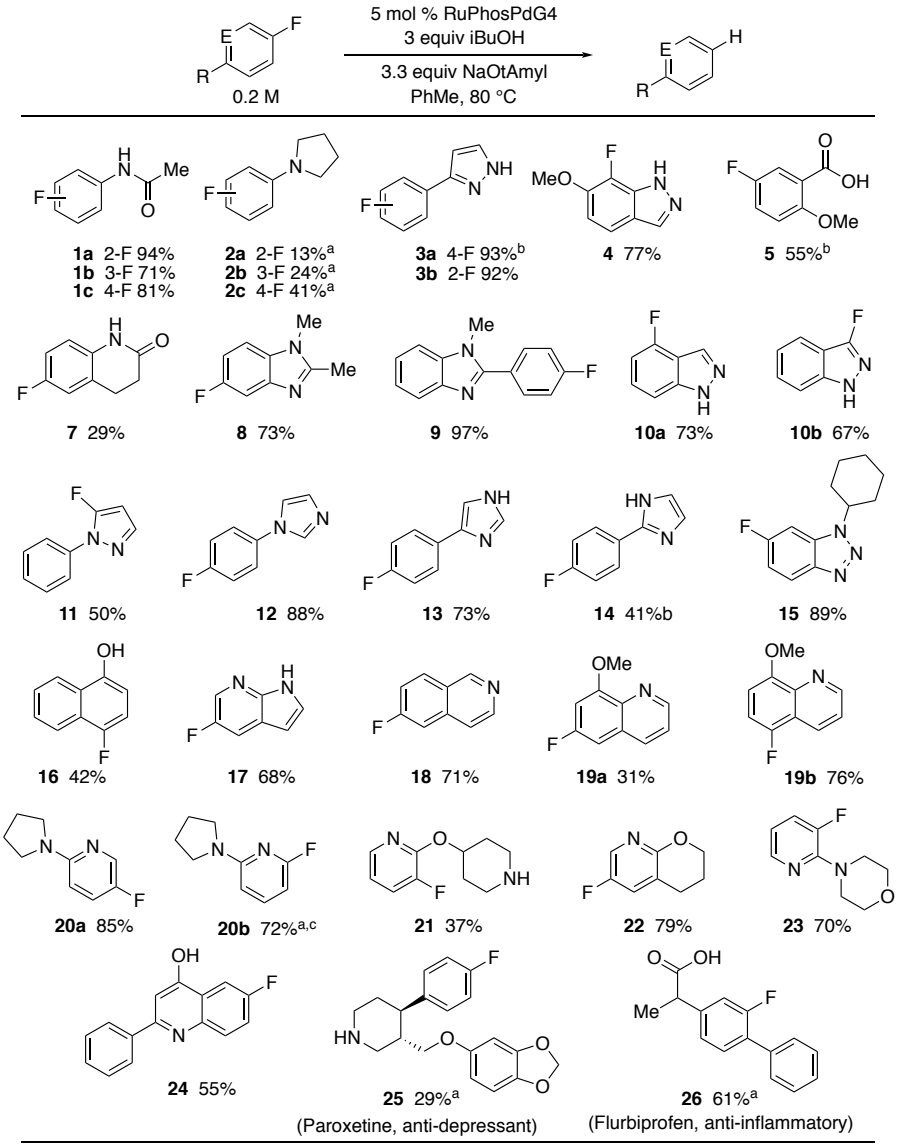

[a]10 mol% Pd, [b]3 mol% Pd, [c]60 °C

References

1. Vertex Pharmaceuticals Inc, 50 Northern Avenue, Boston, MA 02210, USA. Email: Ron_Grey@vrtx.com ORCID 0000-0001-8948-5056.
2. (a) Böhm, H.-J.; Banner, D.; Bendels, S.; Kansy, M.; Kuhn, B.; Müller, K.; Obst-Sander, U.; Stahl, M. *ChemBioChem* **2004**, *5*, 637–643. (b) Kirk, K. L. *J. Fluor. Chem.* **2006**, *127*, 1013–1029. (c) Müller, K.; Faeh, C.; Diederich, F. *Science* **2007**, *317*, 1881–1886. (d) Ricci, P.; Khotavivattana, T.; Pfeifer, L.; Médebielle, M.; Morphy, J. R.; Gouverneur, V. *Chem. Sci.* **2017**, *8*, 1195–1199. (e) Hagmann, W. K. *J. Med. Chem.* **2008**, *51*, 4359–4369. (f) Wang, J.; Sánchez-Roselló, M.; Aceña, J. L.; del Pozo, C.; Sorochinsky, A. E.; Fustero, S.; Soloshonok, V. A.; Liu, H. *Chem. Rev.* **2013**, *114*, 2432–2506. (g) Gillis, E. P.; Eastman, K. J.; Hill, M. D.; Donnelly, D. J.; Meanwell, N. A. *J. Med. Chem.* **2015**, *58*, 8315–8359. (h) Meanwell, N. A. *J. Med. Chem.* **2018**, *61*, 5822–5880. (i) Dimagno, S. G.; Sun, H. *Curr. Top. Med. Chem.* **2006**, *6*, 1473–1482. (j) Smart, B. E. *J. Fluor. Chem.* **2001**, *109*, 3–11.
3. (a) Whittlesey, M. K.; Peris, E. *ACS Catal.* **2014**, *4*, 3152–3159. (b) Amii, H.; Uneyama, K. *Chem. Rev.* **2009**, *109*, 2119–2183. (c) Alonso, F.; Beletskaya, I. P.; Yus, M. *Chem. Rev.* **2002**, *102*, 4009–4092.
4. (a) Tsuzuki, H.; Kamio, K.; Fujimoto, H.; Mimura, K.; Matsumoto, S.; Tsukinoki, T.; Mataka, S.; Yonemitsu, T.; Tashiro, M. *J. Label. Compd. Radiopharm.* **1993**, *33*, 205–212. (b) Maron, L.; Werkema, E. L.; Perrin, L.; Eisenstein, O.; Andersen, R. A. *J. Am. Chem. Soc.* **2005**, *127*, 279–292. (c) Beltrán, T. F.; Feliz, M.; Llusar, R.; Mata, J. A.; Safont, V. S. *Organometallics* **2011**, *30*, 290–297. (d) Chen, Z.; He, C.-Y.; Yin, Z.; Chen, L.; He, Y.; Zhang, X. *Angew. Chem. Int. Ed.* **2013**, *52*, 5813–5817. (e) Senaweera, S. M.; Singh, A.; Weaver, J. D. *J. Am. Chem. Soc.* **2014**, *136*, 3002–3005. (f) Schwartsburd, L.; Mahon, M. F.; Poulten, R. C.; Warren, M. R.; Whittlesey, M. K. **2014**, *33*, 6165–6170. (g) Ekkert, O.; Strudley, S. D. A.; Rozenfeld, A.; White, A. J. P.; Crimmin, M. R. *Organometallics* **2014**, *33*, 7027–7030. (h) Cybulski, M. K.; Riddlestone, I. M.; Mahon, M. F.; Woodman, T. J.; Whittlesey, M. K. *Dalton Trans.* **2015**, *44*, 19597–19605. (i) McKay, D.; Riddlestone, I. M.; Macgregor, S. A.; Mahon, M. F.; Whittlesey, M. K. *ACS Catal.* **2015**, *5*, 776–787. (j) Podolan, G.; Jungk, P.; Lentz, D.; Zimmer, R.; Reissig, H.-U. *Adv. Synth. Catal.* **2015**, *357*, 3215–3228. (k) Liu, X.; Wang, Z.; Zhao, X.; Fu, X. *Inorg. Chem. Front.* **2016**, *3*, 861–865. (l) Matsunami, A.; Kuwata, S.; Kayaki, Y. *ACS Catal.* **2016**, *6*, 5181–5185. (m) Krüger, J.; Leppkes, J.; Ehm, C.; Lentz, D. *Chem. Asian J.* **2016**, *11*, 3062–3071. (n) Mai, V. H.; Nikonov,

G. I. *ACS Catal.* **2016**, *6*, 7956–7961. (o) Cybulski, M. K.; McKay, D.; Macgregor, S. A.; Mahon, M. F.; Whittlesey, M. K. *Angew. Chem. Int. Ed.* **2017**, *129*, 1537–1541. (p) Chen, J.; Huang, D.; Ding, Y. *ChemistrySelect* **2017**, *2*, 1219–1224. (q) Cybulski, M. K.; Nicholls, J. E.; Lowe, J. P.; Mahon, M. F.; Whittlesey, M. K. **2017**, *36*, 2308–2316. (r) Kikushima, K.; Grellier, M.; Ohashi, M.; Ogoshi, S. *Angew. Chem. Int. Ed.* **2017**, *56*, 16191–16196. (s) Matsunami, A.; Kayaki, Y.; Kuwata, S.; Ikariya, T. *Organometallics* **2018**, *37*, 1958–1969. (t) Jaeger, A. D.; Ehm, C.; Lentz, D. *Chem. Eur. J.* **2018**, *24*, 6769–6777. (u) Cybulski, M. K.; Davies, C. J. E.; Lowe, J. P.; Mahon, M. F.; Whittlesey, M. K. *Inorg. Chem.* **2018**, *57*, 13749–13760.

5. (a) Ukisu, Y.; Miyadera, T. ***J***. *Mol. Catal. A Chem.* **1997**, *125*, 135–142. (b) Young, R. J.; Grushin, V. V. *Organometallics* **1999**, *18*, 294–296. (c) Aramendía, M. A.; Borau, V.; Garcíia, I. M.; Jiménez, C.; Marinas, A.; Marinas, J. M.; Urbano, F. J. *Comptes Rendus de l'Académie des Sciences - Series IIC - Chemistry* **2000**, *3*, 465–470. (d) Desmarets, C.; Kuhl, S.; Schneider, R.; Fort, Y. *Organometallics* **2002**, *21*, 1554–1559. (e) Kuhl, S.; Schneider, R.; Fort, Y. *Adv. Synth. Catal.* **2003**, *345*, 341–344. (f) Cellier, P. P.; Spindler, J.-F.; Taillefer, M.; Cristau, H.-J. *Tetrahedron Lett.* **2003**, *44*, 7191–7195. (g) Davies, C. J. E.; Page, M. J.; Ellul, C. E.; Mahon, M. F.; Whittlesey, M. K. *Chem. Commun.* **2010**, *46*, 5151–5153. (h) Wu, J.; Cao, S. *ChemCatChem* **2011**, *3*, 1582–1586. (i) Sawama, Y.; Yabe, Y.; Shigetsura, M.; Yamada, T.; Nagata, S.; Fujiwara, Y.; Maegawa, T.; Monguchi, Y.; Sajiki, H. *Adv. Synth. Catal.* **2012**, *354*, 777–782. (j) Xiao, J.; Wu, J.; Zhao, W.; Cao, S. *J. Fluor. Chem.* **2013**, *146*, 76–79. (k) Sabater, S.; Mata, J. A.; Peris, E. *Nat. Commun.* **2013**, *4*, 1–7. (l) Wu, W.-B.; Li, M.-L.; Huang, J.-M. *Tetrahedron Lett.* **2015**, *56*, 1520–1523. (m) Sabater, S.; Mata, J. A.; Peris, E. *Organometallics* **2015**, *34*, 1186–1190. (n) Xu, Y.; Ma, H.; Ge, T.; Chu, Y.; Ma, C.-A. *Electrochem. Commun.* **2016**, *66*, 16–20. (o) Hokamp, T.; Dewanji, A.; Lübbesmeyer, M.; Mück-Lichtenfeld, C.; Würthwein, E.-U.; Studer, A. *Angew. Chem. Int. Ed.* **2017**, *56*, 13275–13278. (p) Tashiro, M.; Nakamura, H.; Nakayama, K. *Org. Prep. Proced. Int.* **1987**, *19*, 442–446.
6. Gair, J. J.; Grey, R. L.; Giroux, S.; Brodney, M. A. *Org. Lett.* **2019**, *21* (7), 2482–2487.

Appendix
Chemical Abstracts Nomenclature (Registry Number)

Toluene; (108-88-3)
2-Propanol: propan-2-ol; (67-63-0)
Sodium *tert*-pentoxide; (14593-46-5)
3-(4-Fluorophenyl)-1*H*-pyrazole; (154258-82-9)
3-Phenyl-1*H*-pyrazole; (2458-26-6)
RuPhos palladacycle generation 4: Methanesulfonato(2-dicyclohexylphosphino-2',6'-di-i-propoxy-1,1'-biphenyl)(2'-dimethylamino-1,1'-biphenyl-2-yl)palladium(II); (1599466-85-9)

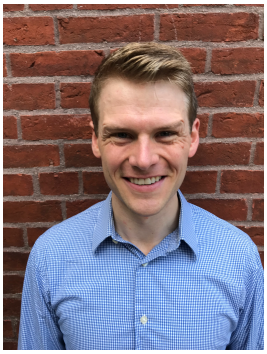

Joseph Gair studied organometallic synthesis with Chris Schaller at Saint John's University, where he earned a B.A. in 2012. Following additional training with Jeffrey Johnson at Hope College, he spent one year teaching secondary school chemistry in Hanga Tanzania with the Benedictine Volunteer Corps. He obtained his Ph.D. from the University of Chicago in 2018 as an NSF research fellow with Jared Lewis. He spent one year as a Co-Op in medicinal chemistry at Vertex Pharmaceuticals before starting his current position as an NIH postdoctoral fellow in the lab of Eric Jacobsen at Harvard University.

Ron Grey received his B.S. in Biochemistry from the University of Delaware in 1997. He subsequently spent 4 years at Dupont's Experimental Station in Wilmington, DE focusing on parallel synthesis. Since 2001, he has served in the Medicinal Chemistry Department at Vertex Pharmaceuticals.

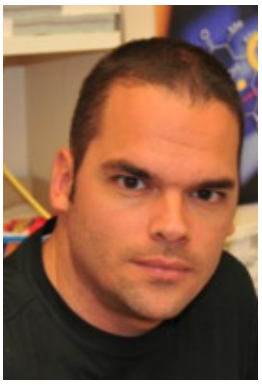

Simon Giroux received his Ph.D. with Prof. Stephen Hanessian from the Université de Montréal in 2006. He subsequently spent 2 years in the laboratory of Prof. E. J. Corey at Harvard University, as an NSERC postdoctoral fellow. He is the author of more than 30 patents and publications and currently serves as a Research Fellow in the Medicinal Chemistry Department at Vertex Pharmaceuticals.

Michael Brodney is currently the Head of Medicinal Chemistry at Vertex Pharmaceuticals. Prior to joining Vertex, Michael was a senior director at Pfizer working on a range of programs in the neuroscience area. He received his Ph.D. with Prof. Al Padwa from Emory University and then moved to Stanford University for an NIH postdoctoral fellowship with Prof. Paul Wender. He is the author of more than 75 patents and publications.

Vincent Porte received his M.Sc in organic chemistry and diploma in Chemical Engineering from the Ecole Nationale Supérieure de Chimie de Montpellier in 2019. During his undergraduate studies, he performed internships in medicinal chemistry and process chemistry at Hoffmann-La Roche and Firmenich. He is currently a second-year graduate student in the group of Prof. Nuno Maulide. His research focuses on the minimization of the flexibility of drug molecules using fused ring systems and the synthesis of natural-product-like structures.

Daniel Kaiser received his Ph.D. at the University of Vienna in 2018, completing his studies under the supervision of Prof. Nuno Maulide. After a postdoctoral stay with Prof. Varinder K. Aggarwal at the University of Bristol, he returned to Vienna in 2020 to assume a position as senior scientist in the Maulide group. His current research focusses on the chemistry of destabilized carbocations and related high-energy intermediates.

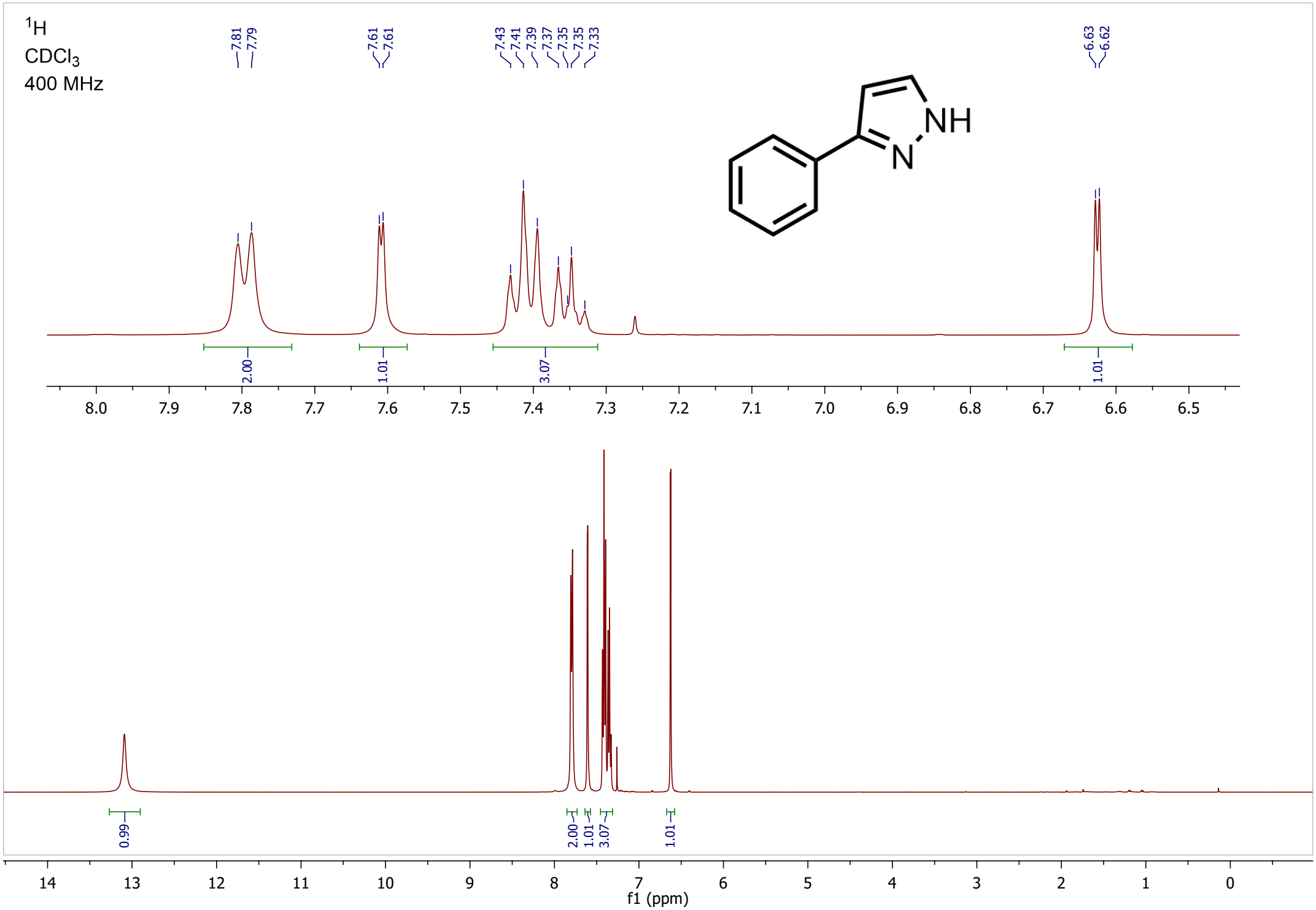
1H
CDCl3
400 MHz
7.81
7.79
7.61
7.61
7.43
7.41
7.39
7.37
7.35
7.35
7.33
6.63
6.62
NH
N
2.00
1.01
3.07
1.01
0.99
2.00
1.01
3.07
1.01
f1 (ppm)

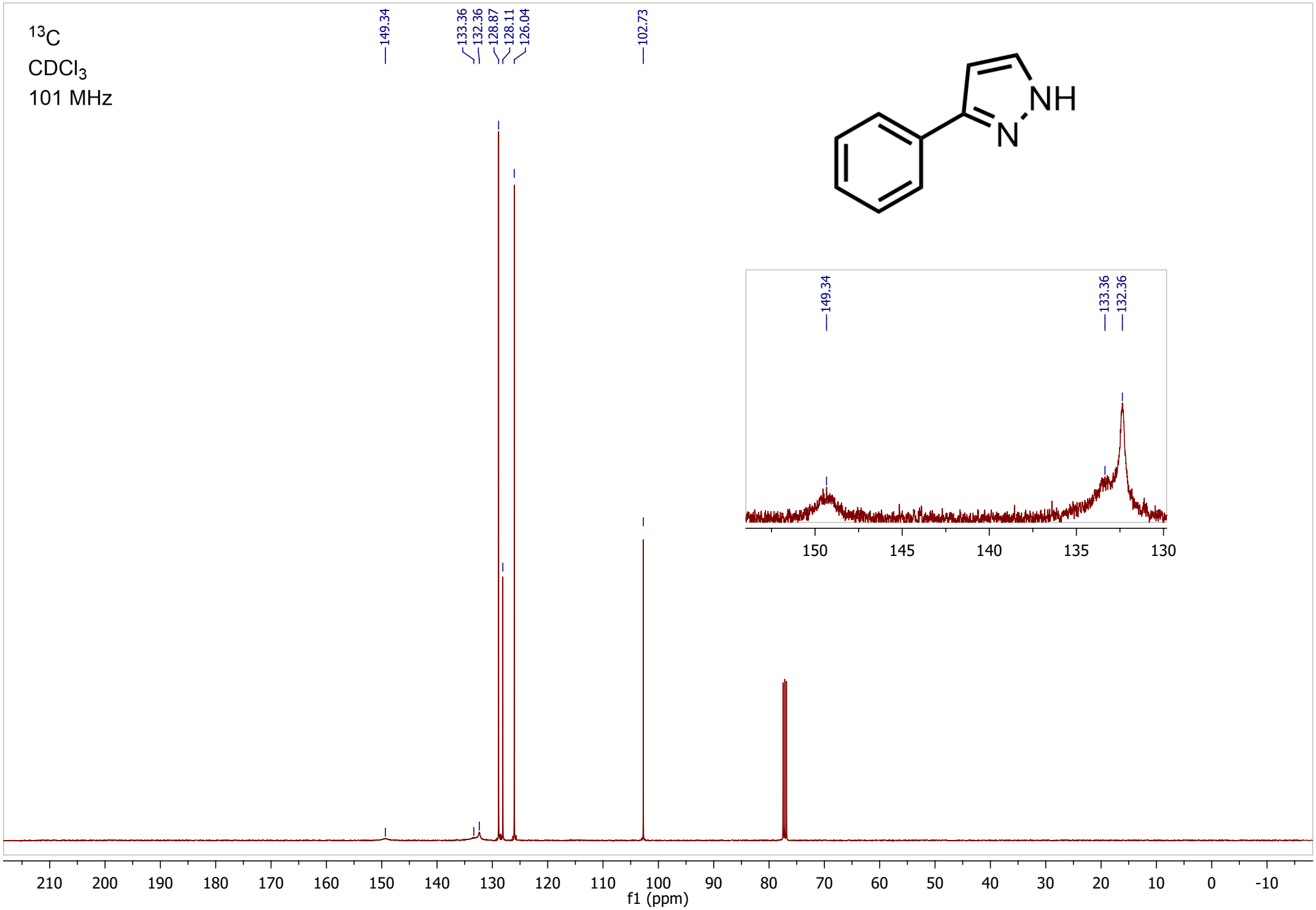
^{13}C
$CDCl_3$
101 MHz
149.34
133.36
132.36
128.87
128.11
126.04
102.73
NH
N
149.34
133.36
132.36
150
145
140
135
130
210
200
190
180
170
160
150
140
130
120
110
100
90
80
70
60
50
40
30
20
10
0
-10
f1 (ppm)

^1H
$CDCl_3$
400 MHz